

# Investigation into the compression behaviour of unsaturated damaged Callovo-Oxfordian claystone

Hao Wang<sup>1\*</sup>, Yu-Jun Cui<sup>1</sup>, Minh-Ngoc Vu<sup>2</sup>, and Jean Talandier<sup>2</sup>

<sup>1</sup>Ecole des Ponts ParisTech, Laboratoire Navier/CERMES, 6 et 8 avenue Blaise Pascal, 77455 Marne La Vallée cedex 2, France

<sup>2</sup>Andra, R&D Department, 92290 Châtenay-Malabry, France

**Abstract.** In this study, the compression behaviour of unsaturated damaged COx claystone is investigated by performing high pressure oedometer tests with controlled suction. The damaged oedometer samples were prepared by shearing the claystone in triaxial conditions. Four high pressure oedometer tests were conducted using different controlled suctions. The effects of suction and damage on the swelling and compression were investigated in oedometer. Results show that the intact claystone exhibits a larger swelling strain than that of the damaged one at the same imposed suction. The damaged claystone at a lower suction displays a smaller yield stress and higher compressibility, and exhibits a larger compression index  $C_c$  than the intact one, evidencing the effect of damage. In addition, the step compression index  $C_c^*$  increases with the increase of vertical stress, while decreases with the decrease of suction. This indicates the dependencies of compression behaviour on vertical stress and suction.

## 1 Introduction

In France, an Underground Research Laboratory (URL) was constructed by the French national agency for the management of nuclear waste (ANDRA) at Bure in the Callovo-Oxfordian claystone (COx) formation at the depth between 420 and 550 m [2]. Damages were induced by the excavation of shafts and drifts inside the COx claystone formations, named excavation damaged zone (EDZ). This has unfavourable effects on the mechanical behaviours of COx claystone [3, 15, 16]. Armand et al. [3] reported that the convergence of the drifts was affected by the pattern and the density of fractures in EDZ. Moreover, unsaturation in COx claystone was also induced by the ventilation in URL [4]. In this case, it is important to well understand the hydro-mechanical behaviour of damaged COx claystone for estimating the safety performance of potential repository.

To date, a large number of laboratory investigations has been performed to characterise the effect of damage on the hydro-mechanical behaviour of COx claystone [19, 25-28]. In the swelling aspect, Zhang et al. [25-27] investigated the gas and water permeabilities of artificially fractured COx claystone with consideration of the swelling of clay minerals (e.g., interstratified illite/smectites, illite, and kaolinite) inside COx claystone induced [13, 23]. The pre-existing fractures were filled and clogged by swollen clay minerals, significantly reducing the permeability of fractured COx claystone, i.e., self-sealing, as reported by Giot et al. [10]. and Di Donna et al. [9] through X-ray computed tomography (CT). However, the investigations mainly focused on

the swelling behaviour of fractured COx claystone at saturated state.

In terms of the volumetric compression behaviour, few studies were carried out [12, 13, 19]. Mohajerani et al. [12] presented that microcracks occurred when unloaded from a high stress, showing the increase of the swelling capacity. Wang et al. [19] investigated the compression behaviour of COx claystone with different fracture orientations. It appears that the orientation of fracture and the applied stress significantly affected the volume change property. The water permeability decreased during loading because of the closure of the fracture zone. Chiarelli et al. [6] and Zhang et al. [27] reported that significant plastic volumetric strain and anisotropy were observed on COx claystone under isotropic compression. Until now, there is few investigations into the swelling and compression of unsaturated damaged COx claystone.

In this study, the swelling and compression behaviour of unsaturated damaged COx claystone was investigated. The damaged COx claystone was prepared using the method proposed by Wang et al. [20]. Suction-controlled oedometer tests were conducted on damaged COx claystone to investigate the swelling and compression behaviours. Based on the results obtained, the compression parameters were analysed, allowing the further understanding of the influence of suction on the compression behaviour of unsaturated and damaged COx claystone.

\* Corresponding author: [hao.wang@enpc.fr](mailto:hao.wang@enpc.fr)

## 2 Materials and methods

### 2.1 Materials

In this study, the used COx claystone was obtained from the URL at Bure, France, with the in-situ stresses of: ~12.7 MPa in the vertical direction, ~12.7-14.8 MPa in the major horizontal stress direction, ~12.4 MPa in the minor horizontal stress direction, with a pore water pressure of 4.7 MPa [22]. Clay minerals account for 50-55%, including 30% illite, 15% kaolinite and chlorite and 55% interstratified illite/smectite in the mineral composition. It also contains tectosilicates (20%), carbonates (20%–25%), pyrite and iron oxides (3%) [2]. The used COx claystone core was preserved in T1 cell for keeping the water content and minimising the decompression induced by unloading [7]. In the present study, the used COx core was from T1 cell EST58107. The basic parameters were determined and shown in Table 1. The detailed determination method can be found in Wang [18].

**Table 1.** Initial characteristics of COx claystone core.

Index	Value
Bulk density (Mg/m <sup>3</sup> )	2.40
Porosity (%)	17.9
Water content (%)	8.06
Initial suction (MPa)	20.33

### 2.2 Sample preparation

A triaxial sample with diameter of 38 mm was first prepared with the axial direction perpendicular to the bedding plane, then sawed using a diamond line to a designed height of 65 mm. To obtain damaged oedometer samples, the triaxial sample was first artificially sheared in high pressure triaxial cell. For this purpose, normalized tangent Young modulus  $E_T/E_I$  was used as the damage indicator ( $E_I$ : initial Young modulus,  $E_T$ : the tangent Young modulus in the axial direction), recommended by Wang et al. [20]. The preparation of damaged oedometer samples contains three steps: (i) to select a reasonable ratio of  $E_T/E_I$  for ensuring that damage can be produced; (ii) to shear a triaxial sample in triaxial cell to the selected value of  $E_T/E_I$  under constant mean stress condition [11]; (iii) to unload the sample, then cut it. In this study, the triaxial sample was first isotopically loaded to the confining pressure of 14 MPa at a loading rate of 100 kPa/min, then a constant mean stress loading path was adopted for the shearing at an axial strain rate of  $6 \times 10^{-6}/s$ , as recommended by Zhang et al. [27] and Liu et al. [11]. A typical loading-unloading curve is presented in Fig. 1. A value 0.22 of  $E_T/E_I$  was selected, corresponding to almost 0.9 time the

peak deviator stress [18]. This stress is larger than the crack initiation one (0.6 time the peak deviator stress) and the dilatant one (0.83 time the peak deviator stress) identified by Zhang et al. [26], ensuring the presence of damage-induced micro-cracks inside the triaxial sample. Wang et al. [20] reported that the distribution of micro-cracks was inhomogeneous through CT scanning due to the effect of friction close to the top and bottom of sample. Thus, four damaged oedometer samples were cut into the designed dimension (38 mm in diameter and 10 mm in height) from the central part of the damaged triaxial sample.

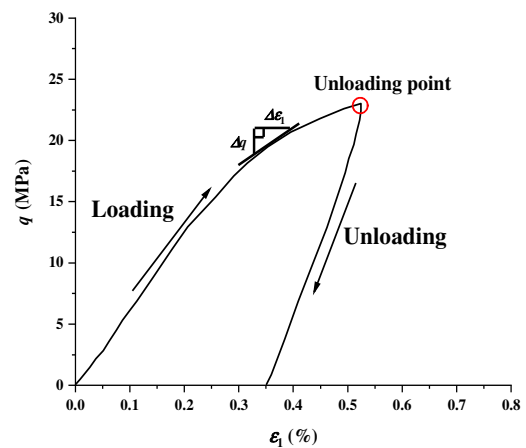


**Fig. 1.** Typical stress-strain curve from triaxial test.

### 2.3 Experimental methods

To investigate the compression behaviour of damaged COx claystone, four high pressure oedometer tests under different controlled suctions (0 MPa, 4.2 MPa, 9 MPa and 24.9 MPa) were carried out. The experimental setup is shown in Fig. 2. The experimental procedure contains two stages: suction equilibration and step-loading. For the suction equilibration, the samples were firstly installed in oedometer cells, then equilibrated at the designed suctions (0 MPa, 4.2 MPa, 9 MPa and 24.9 MPa). Synthetic water was used for imposing zero suction, as reported by Wang et al. [20]. Note that the used synthetic water in this study has a quite low electrical conductivity ( $6.3 \mu S/cm$ ), corresponding to an osmotic suction of 0.1 MPa. This was ignored in this work. Other saturated salt solutions ( $K_2SO_4$ ,  $KNO_3$  and  $(NH_4)_2SO_4$ ) were used for non-zero suctions by the Vapour Equilibrium technique (VET), corresponding to 4.2 MPa, 9 MPa and 24.9 MPa, respectively. During the suction application, an initial vertical stress of 0.05 MPa was applied to make a good contact between the piston and sample. Suction equilibrium was considered as reached when the vertical strain rate was below 0.025%/day, as recommended by Romero et al. [14].

During loading process, the damaged oedometer sample was loaded in steps from a stress of 0.125 MPa to a maximum stress of 64 MPa by keeping the current stress double of the previous one and the suction constant. The vertical strain under each load was considered as stabilized, when the primary

consolidation was finished [5]. In addition, COx claystone shows a gradual yielding property with stress, thus the step compression index  $C_c^*$  is determined to investigate the change in compressibility with stress, as reported by Wang et al. [19].

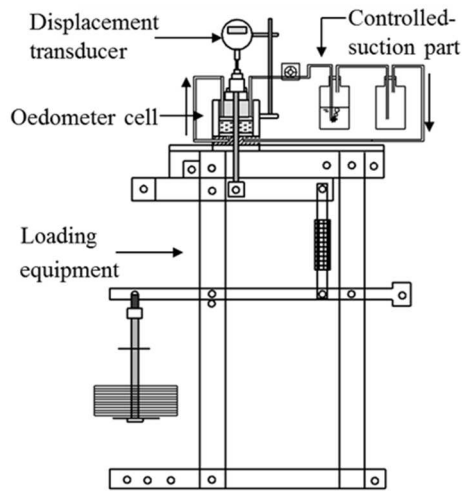


**Fig. 2.** Experimental setup for suction-controlled oedometer tests.

### 3 Results and discussions

Fig. 3 presents the evolution of vertical strain (positive denoting swelling) with time during suction equilibration for the four tests. It is observed that the test at a higher suction shows a lower vertical swelling strain and needs less time for suction equilibrium. This is consistent with the observations on other unsaturated soils [21]. The final strains obtained for suctions of 0 MPa, 4.2 MPa, 9 MPa, and 24.9 MPa are 2.01%, 0.61%, 0.33% and 0.03%, respectively.

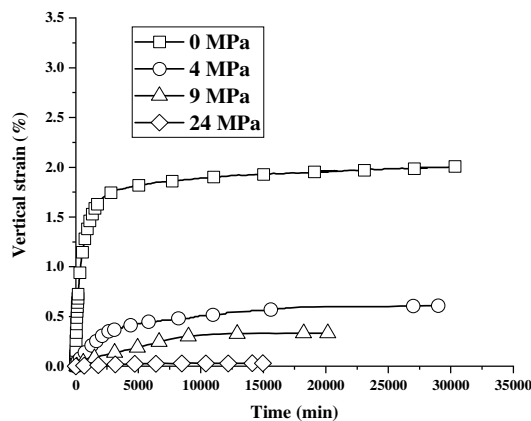


**Fig. 3.** Evolution of vertical strain with time during suction equilibration.

Fig. 4 presents the comparison between the vertical swelling strains obtained in this study and those from other works. Results show that a relative linear relationship is obtained between strain and suction for both the damaged claystone in this study and the intact claystone by Menaceur et al. [13] and Wang [18]. For the intact claystone, the samples were hydrated under free swelling [13], while an initial vertical stress of

0.05 MPa was applied in the oedometer swelling condition [18]. Thus, the former show higher volumetric strains than the latter at low suctions, indicating the stress-dependence of swelling behaviour of COx claystone. In addition, it appears that the damaged claystone presents lower swelling strain than the intact claystone by Wang [18]. The difference is attributed to the effect of micro-cracks inside the damaged claystone. Due to the filling of swollen clay minerals in the micro-cracks, the overall swelling potential decreases. This is similar to the fracture effect on the swelling behaviour of fractured COx claystone [19, 28].

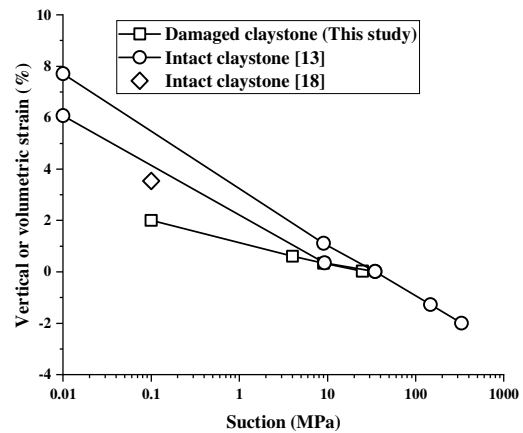


**Fig. 4.** Vertical or volumetric strain versus suction after suction equilibration.

After suction equilibration, the claystone samples were loaded in steps at constant suctions. Fig. 5 presents the compression curves at different suctions in terms of void ratio with respect to the logarithm of vertical stress. Note that the initial void ratios before swelling were slightly different due to the claystone variability. It appears that based on the compression curves, the sample at a higher suction displays a lower compressibility due to the suction hardening effect of unsaturated soils. The compression curves can be generally divided into two parts: an elastic part with low compressibility before the yield stress and a plastic part with high compressibility after the yield stress. However, for test at zero suction, the compression curve deviates from the linear relation after 16 MPa, generating a third part with a higher compressibility. This phenomenon was attributed to the grain breakage effect by Wang et al. [17].

The yield stress at each suction was identified using the bilinear method based on the elastic part and the plastic one shown in Fig. 5. For zero suction, the plastic part is well identified with the middle linear part, while the part corresponding to the last two loading steps was regarded as the plastic one based on the nonlinearity of the compression curves for the other three suctions. Fig. 6 shows the changes in yield stress with respect to suction. It is observed that for the damaged claystone, the yield stress increases with the increase of suction. This observation is in agreement with that on other unsaturated soils [1].

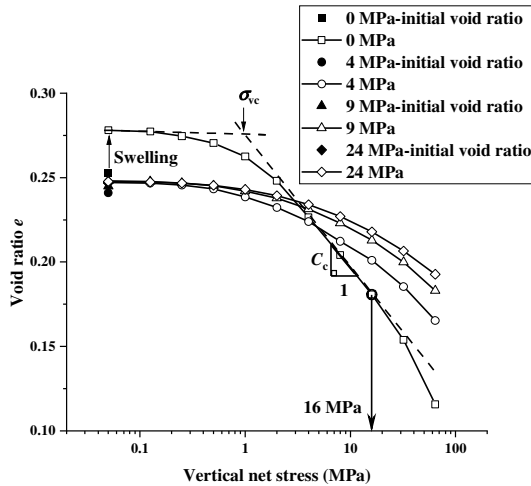


**Fig. 5.** Compression curves at different suctions.

The determination of the compression coefficient  $C_c$  is also depicted in Fig. 5. Fig. 7 displays the evolution of  $C_c$  with respect to suction. As observed,  $C_c$  decreases almost linearly with the increase of suction. Comparison of  $C_c$  at zero suction shows that the damaged claystone has a significantly larger  $C_c$  than the intact claystone due to the influence of existing micro-cracks inside the damaged sample. Menaceur et al. [13] reported that large pores/micro-cracks were created inside intact claystone due to the damage induced by the swelling of clay minerals in the hydration process. The combined contributions of the pre-existing micro-cracks and the induced ones increased the compressibility of damaged claystone in the second plastic part (Fig. 5), similar to the observations on fractured claystone by Wang et al. [19].

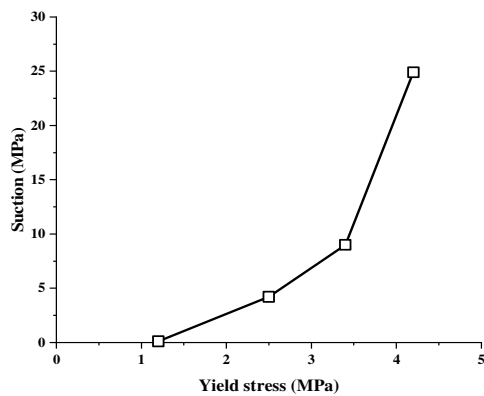


**Fig. 6.** Relationship between yield stress and suction.

To further investigate the suction effect on the compression behaviour of damaged claystone, the relationships between step compression index  $C_c^*$  and vertical net stress at different suctions are determined as shown in Fig. 8. The determination method for the parameter is the same as in that by Deng et al. [8] and Wang et al. [17].

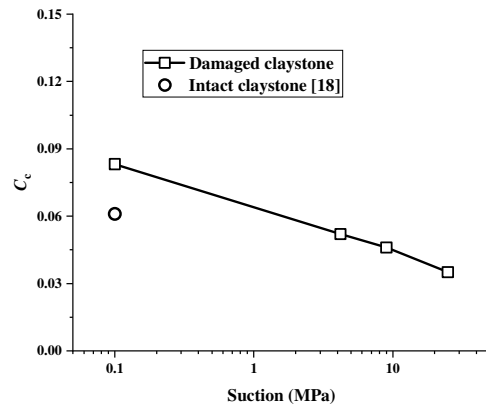


**Fig. 7.** Changes in  $C_c$  with suction.

From Fig. 8, it is found that with the increase of vertical stress,  $C_c^*$  shows an increasing tendency at suctions 4.2 MPa, 9 MPa and 24.9 MPa. However, at suction zero,  $C_c^*$  increases first, then changes little with vertical stress, finally significantly increases after 16 MPa. Wang et al. [19] reported that compared with intact claystone, the evolution of  $C_c^*$  of fractured claystone is influenced by the collapse of large pores in the fracture zone before 16 MPa, reflecting the effect of existing fracture. However, after 16 MPa,  $C_c^*$  keeps increasing with the increase of vertical stress, which is attributed to the contributions of grain breakage to the compressibility of claystone [19]. Thus, it is inferred that the evolution of  $C_c^*$  of damaged claystone with vertical stress follows the same mechanism, as reported by Wang [18]. However, under other suctions, this phenomenon is not obvious. It is attributed to the increase of the stiffness of clay matrix due to the increase of suction. In that case, the contribution of the collapse of large pores to  $C_c^*$  is reduced and only the continuous increasing tendency can be observed. Besides, in a standard fashion, larger  $C_c^*$  was observed for lower suction at the same stress. This shows the dependency of compression behaviour of damaged claystone on suction and stress.

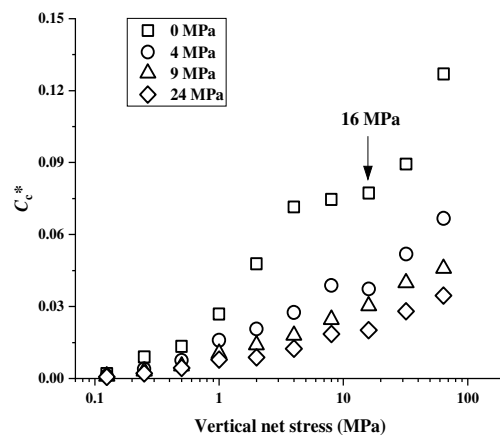


**Fig. 8.**  $C_c^*$  versus vertical net stress.

## 4 Conclusions

In this study, the compression behaviour of damaged COx claystone was investigated. Four oedometer tests with controlled-suction were performed on damaged COx claystone. Based on the obtained results, the following conclusions can be drawn:

In oedometer tests with controlled suction, the damaged claystone shows a slightly lower swelling strain than the intact claystone. This is attributed to the swollen clay minerals which filled the pre-existing micro-cracks inside the damaged claystone, leading to a decrease of the swelling potential. Besides, in a standard fashion, the damaged claystone with a higher suction exhibits a lower compressibility and larger yield stress. Compared with the intact claystone, the damaged one presents a lower compression index  $C_c$ .  $C_c^*$  also increases with the increase of vertical stress and with the decrease of suction, showing the dependence of the compression behaviour on stress and suction. Note that 16 MPa is a key stress for COx claystone, which is related to the closure of micro-cracks and grain breakage.

## References

1. E.E. Alonso, A. Gens, A. Josa, *Géotechnique* **40**, (1990)
2. G. Armand, A. Noiret, J. Zghondi, D.M. Seyedi, J. Rock Mech. Geotech. Eng. **5** (2013).
3. G. Armand, F. Leveau, C. Nussbaum, R. de La Vaissière, A. Noiret, D. Jaeggi, P. Landrein, C. Righini, *Rock Mech. Rock. Eng.* **47** (2014)
4. G. Armand, H. Djizanne, J. Zghondi, R. de La Vaissière, J. Talandier, N. Conil, *Inputs from in situ experiments to the understanding of the unsaturated behaviour of Callovo-Oxfordian claystone*, In E3S Web of Conferences (EDP Sciences, 2016)
5. ASTM, D2435-96., ASTM International (1996)
6. A. S. Chiarelli, J.F. Shao, N. Hoteit, *Int. J. Plast.* **19** (2003)
7. N. Conil, J. Talandier, H. Djizanne, R. de La Vaissière, C. Righini-Waz, C. Auvray, C. Morlot, G. Armand, *J. Rock Mech. Geotech. Eng.* **10** (2018).
8. Y.F. Deng, Y.J. Cui, A.M. Tang, X.L. Li, X. Sillen, *Appl Clay Sci.* **59**(2012)
9. A. Di Donna, P. Charrier, S. Salager, P. Bésuelle, *Self-sealing capacity of argillite samples*, In E3S Web of Conferences (EDP Sciences, 2019)
10. R. Giot, C. Auvray, J. Talandier, *Self-sealing of claystone under X-ray nanotomography*. Geological Society Special Publications, London, **482** (2019)
11. Z. Liu, J. Shao, S. Xie, N. Conil, J. Talandier, *Rock Mech. Rock Eng.* **52** (2019)
12. M. Mohajerani, P. Delage, M. Monfared, A.M. Tang, J. Sulem, B. Gatmiri, *Int. J. Rock Mech. Min. Sci.* **48** (2011)
13. H. Menaceur, P. Delage, A.M. Tang, J. Talandier, *Rock Mech. Rock. Eng.* **49** (2016)
14. E. Romero, A. Gens, A. Lloret, *Géotechnique* **53** (2003)
15. D. M. Seyedi, G. Armand, A. Noiret, *Comput. Geotech.* **85** (2017)
16. M.N., Vu, L.M. Guayacán Carrillo, G. Armand, *Eur J Environ Civ En*, 1-16 (2020)
17. H. Wang, Y.J. Cui, F. Zhang, J.J., Liu, *Acta Geotech.* 1-10. (2021)
18. H. Wang, *Delayed and Swelling Behaviour of Damaged/Fractured Callovo-Oxfordian Claystone*, Doctoral dissertation, Marne-la-vallée, ENPC (2021)
19. H., Wang, Y.J., Cui, M.N., Vu, J. Talandier, N. Conil, *Eng. Geol.* **303** (2022).
20. H., Wang, Y.J., Cui, M.N., Vu, J. Talandier, N. Conil, *Rock Mech. Rock Eng.* **55**(10) (2022)
21. Q., Wang, A.M. Tang, Y.J. Cui, P. Delage, J.D. Barnichon, W.M. Ye, *Soils Found.* **53** (2013)
22. Y. Wileveau, F.H. Cornet, J. Desroches, P. Blumling, *Phys. Chem. Earth.* **32** (2007)
23. B. Yven, S. Sammartino, Y. Geraud, F. Homand, F. Villieras, *Mineralogy, texture and porosity of Callovo-Oxfordian argillites of the Meuse/Haute-Marne region (eastern Paris Basin)*. Mémoires de la Société géologique de France, **178** (2007)
24. C.L. Zhang, *Self-sealing of fractures in argillites under repository conditions*, In International conference and workshop in the framework of the EC TIMODAZ and THERESA projects (2009)
25. C.L. Zhang, *J. Phys. Chem. Earth.* **36** (2011)
26. C.L. Zhang, *J. Rock Mech. Geotech. Eng.* **5** (2013)
27. C.L. Zhang, G. Armand, N. Conil, B. Laurich, *Eng. Geol.* **251** (2019)
28. F. Zhang, Y.J. Cui, N. Conil, J. Talandier, *Eng. Geol.* **280** (2021)